Splitting, return maps and confined motion in the planar RTBP: Theory and praxis

Carles Simó

Dept. Matemàtica Aplicada i Anàlisi, UB, Barcelona, Catalunya

carles@maia.ub.es

Edinburgh Mathematical Society -

Societat Catalana de Matemàtiques

joint meeting

Barcelona, 28-30 May 2015

The problem

Many phenomena are described using a **Hamiltonian formulation**. **Integrable cases** can be useful approximations.

We want to present some of the **simplest cases** described by a **Hamiltonian** and the related **Poincaré maps**. For simplicity we restrict to **2 dof Hamiltonian systems** and the related **2D symplectic maps**.

A key question:

Assume an integrable system has a **separatrix** which is **broken** when adding a **perturbation**. Can we give **realistic quantitative estimates** on the **location of invariant curves** for the 2D map based on **theoretical considerations** and some information on **geometrical objects**?

In this context a **key role is played by return maps**, like the **separatrix map** and **related maps**, like the **standard map**.

Unless otherwise said, we work in the **analytic** context.

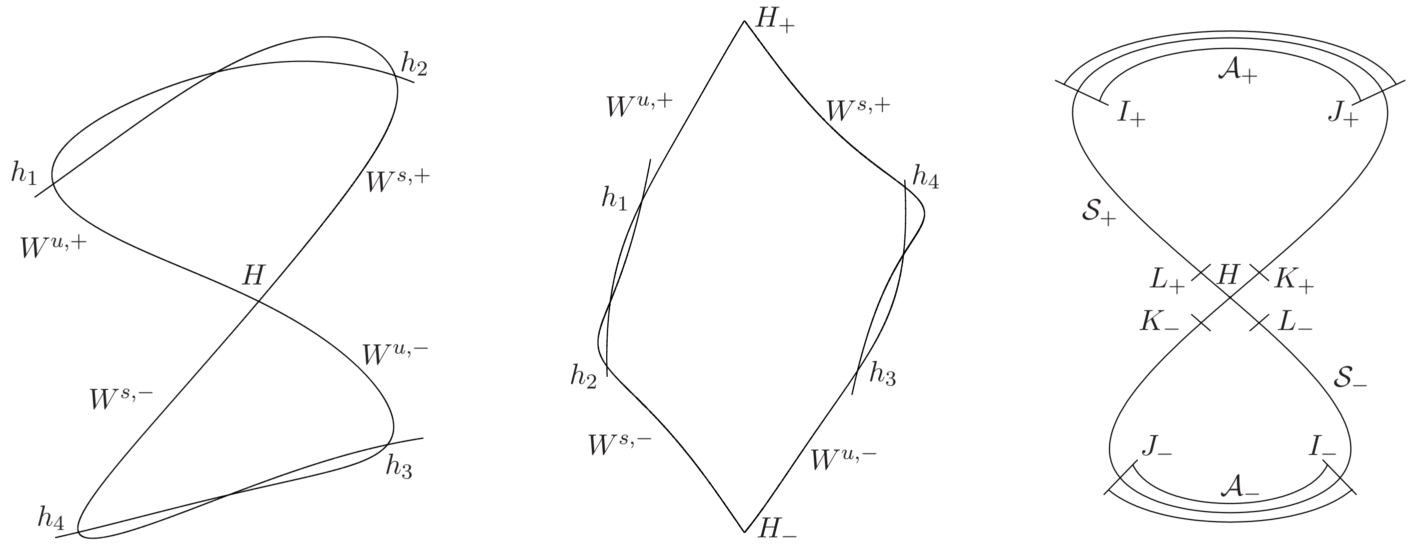

Models for the **homoclinic** (left) and **double heteroclinic** (middle) connections for maps F_ε giving rise to **return maps**. Right plot: an **integrable homoclinic** (e.g.: time-T of the flow of a 1 dof Hamiltonian).

Integrable case (right): Any orbit passing **close to H** (not in W^s) **returns to $\mathcal{A}_+ \cup \mathcal{A}_-$**. Assume $F_0(I_\pm) = J_\pm$. In the left and middle case **one takes $I_\pm$ transversal to W^u through h_1, h_3**.

Let F_ε be **ε-close to the identity** with **dominant eigenvalue at H $\lambda(\varepsilon) = 1 + \mathcal{O}(\varepsilon)$** and $\gamma(\varepsilon) = \log(\lambda(\varepsilon))/(2\pi)$. The map **can be approximated by the 2π-time flow of a 1 dof slow Hamiltonian** $\gamma(\varepsilon)\,\mathcal{H}$ with error **exponentially small in ε**, as follows from **suspension and averaging**.

Return maps: Model the **first return to $\mathcal{A}_+ \cup \mathcal{A}_-$** (if it exist) after passing close to H. In present context known as **separatrix maps**.

Integrable case: 2π-map of a 1 dof Hamiltonian. Use (t,h) as **coordinates in $\mathcal{D}$**, with t counted from I, $h=0$ on the separatrix, $h>0$ inside the loop, being h the energy level of $\mathcal{H}$. Let $T(h,\varepsilon)$ be the **period under $\gamma(\varepsilon)\mathcal{H}$**: $T(h,\varepsilon)=c_0+|\log(h)|/\gamma(\varepsilon)+\mathcal{O}(h,\varepsilon)$.

The separatrix map is $SepM:\begin{pmatrix} t \\ h \end{pmatrix} \to \begin{pmatrix} \bar{t}=t-T(h,\varepsilon) \pmod{2\pi} \\ \bar{h}=h \end{pmatrix}.$

The general map case F_ε: We should take into account the **splitting of the separatrices**. Let $a(\varepsilon)\,\xi(t)$ the **position, in energy, of W^u wrt W^s** in $\mathcal{D}$. The value $a(\varepsilon)$ measures the **amplitude** of the splitting and $\xi(t)$ is a **normalized shape**. Then

$$SepM:\begin{pmatrix} t \\ h \end{pmatrix} \to \begin{pmatrix} \bar{t}=t-c_0-|\log(\bar{h})|/\gamma(\varepsilon)+\mathcal{O}(h) \pmod{2\pi} \\ \bar{h}=h+a(\varepsilon)\xi(t) \end{pmatrix}.$$

For the **classical separatrix map** $\xi(t)=\sin(t)$.

Basic ingredients for a return map:

The return time from $\mathcal{A}_+ \cup \mathcal{A}_-$ to itself, which can be of $T_+, T_-, T_\pm$ or $T_\mp$ type and, in turn **depends of the character of H, e.g., hyperbolic or parabolic**.

The splitting of the separatrices, which in some problems can be **exponentially small in some small parameter**.

Several persons have done and/or are doing work on **regularity of manifolds, splitting, return maps and applications** inside the **UB-UPC Dynam. Systems Group**. A (non-exhaustive) list of names is:

Baldomà, I., Benseny, A., Cabré, X., Canadell, M., Canalías, E., Castejón, O., Delshams, A., Fontich, E., Gómez, G., Guardia, M., Gutiérrez, P., Haro, À., Huguet, G., Jorba, À., Llibre, J., Martín, P., Martínez, R., Martínez-Seara, T., Masdemont, J., Miguel, N., Mondelo, J.M., Olivé, C., Ollé, M., Ramírez, R., Roldán, P., Tatjer, J.C., Valls, C., Vieiro, A., with collaborators of many research centers from abroad.

Return maps are **useful tools to understand many dynamical properties**.

In turn the classical $SepM$ can be approximated around $h = h_0$ if $h_0 \geq a(\varepsilon)/\gamma(\varepsilon)$, by the **classical standard map** (Chirikov) in $\mathbb{T}^2$.

$$SM_\kappa : \begin{pmatrix} u \\ v \end{pmatrix} \to \begin{pmatrix} \bar{u} = u + \bar{v} \\ \bar{v} = v + \kappa \sin(u) \end{pmatrix}, \quad \text{where} \quad \kappa = a(\varepsilon)/(h_0\gamma(\varepsilon)).$$

For $\kappa > \kappa_G \approx 0.971635406$ **(Greene's value)** SM_κ has some **chaotic dynamics with v unbounded**. This occurs for $h_0 < a(\varepsilon)/(\kappa_G\gamma(\varepsilon))$.

For η small, fixed, **upper bounds for $a(\varepsilon)$** are of the form (Fontich-S) $N(\eta)\exp(-(c-\eta)/\gamma(\varepsilon))$, where c is the **smallest distance to the real line of the singularities of the separatrix of $\mathcal{H}$**.

A more accurate study gives in many problems

$$a(\varepsilon) = A\varepsilon^B \exp(-c/\gamma(\varepsilon))(1 + \mathcal{O}(\varepsilon)),$$

for suitable A, B, which implies **most of the chaos is confined to a domain of size**

$$\approx A^*\varepsilon^{(B-1)} \exp(-c/\gamma(\varepsilon)).$$

Note: **big changes when sin is replaced by another normalized periodic function**.

The planar RTBP case

It describes the motion of a **massless body** under the action of **bodies of masses $1-\mu, \mu$** moving in **circular orbits** around the c.o.m. In a fixed frame the dynamics is described by

$$H(X_1, X_2, Y_1, Y_2, t) = \frac{1}{2}(Y_1^2 + Y_2^2) - \left(\frac{1-\mu}{r_1} + \frac{\mu}{r_2}\right),$$

where (X_1, X_2) is the position of the small body in an inertial frame and

$$r_1^2 = (X_1 - \mu\cos(t))^2 + (X_2 - \mu\sin(t))^2, \quad r_2^2 = (X_1 + (1-\mu)\cos(t))^2 + (X_2 + (1-\mu)\sin(t))^2.$$

It has 2 d.o.f., is 2π-time periodic and a **first integral (Jacobi)** given as $C = 2(M-H)$, $M = X_1Y_2 - X_2Y_1$ and H as before.

For μ small is a perturbation of the 2BP.

In the 2BP there are **parabolic orbits on $H=0$**. Can be seen as a **fixed point of parabolic type** in suitable coordinates, usually called **fixed point at infinity**. The manifolds W^u **and** W^s **coincide**.

In the planar RTBP: the fixed point becomes **a periodic orbit at infinity**. The manifolds **do not longer coincide**. The lack of coincidence leads to well-known facts: **non-integrability, existence of symbolic dynamics and oscillatory solutions, escape and capture domains, etc**.

At some distance of $W^{u,s}$ in a suitable **Poincaré section (e.g., pericenter passage)** one can expect **invariant rotational curves (IRC) confining the dynamics**.

Present goals

To study the **infinity manifolds, the related splitting and the dependence in (μ, C)**.
To compare **theory and praxis** as a source of **new problems and deeper understanding**.
To detect numerically **boundaries preventing escape (and capture) as a function of (μ, C)**.

Some strongly related references of the team on that topic:

J. Llibre, Evoluciones finales y movimientos cuasialeatorios en el problema restringido de tres cuerpos, Ph.D., 1979.

J. Llibre and C. Simó, Oscillatory solutions in the planar restricted three-body problem. Math. Ann., 248:153–184, 1980.

A. Benseny, Contribució a l'estudi del problema restringit de tres cossos, Ph.D., 1984.

R. Martínez and C. Pinyol, Parabolic orbits in the elliptic restricted three-body problem. Journ. Diff. Equations, 111:299–339, 1994.

R. Martínez and C. Simó, The invariant manifolds at infinity of the RTBP and the boundaries of bounded motion. Regular and Chaotic Dynamics, 19:745–765, 2014.

M. Guardia, P. Martín and T. M.Seara, Oscillatory motions for the restricted planar circular three-body problem. Invent. math. DOI 10.1007/s0022-015-0591-y, 2015.

Some comments on the Poincaré section

We use the **pericenter passage**

$\Sigma = \{(X_1, X_2, Y_1, Y_2, t) \in \mathbb{R}^5 \mid r = (X_1^2 + X_2^2)^{1/2}$ local minimum wrt $t\}$.

Two-body problem: Given C and $h = 0$, we have for the pericenter distance the value $r_p = C^2/8$. But ...

If $h \neq 0$, from $M = C/2 + h$ and using $M = r_p v_p$ (v_p = velocity at the pericenter)

$$h = (C/2 + h)^2/(2r_p^2) - 1/r_p$$

allows to obtain r_p. Let $r_p = C^2/8 + \Delta$ around $h = 0$.
For the **critical value** $C = C_c = 32^{1/3}$ one has $\Delta = h^2/2 + \mathcal{O}(h^3)$.
For $C \neq C_c$ one has $\Delta = -(C^4/64 - C/2)h + \mathcal{O}(h^2)$.

This will produce **anomalous effects on the splitting**.

Invariant manifolds at infinity

In a **synodical (rotating) frame**

$$\ddot{x} - 2\dot{y} = \frac{\partial\Omega}{\partial x}, \qquad \ddot{y} + 2\dot{x} = \frac{\partial\Omega}{\partial y},$$

$$\Omega(x,y) = \frac{1}{2}(x^2+y^2)+\frac{1-\mu}{r_1}+\frac{\mu}{r_2}, \quad r_1^2 = (x-\mu)^2+y^2, \quad r_2^2 = (x+1-\mu)^2+y^2$$

with **Jacobi constant** $C = 2\Omega(x,y) - (\dot{x}^2 + \dot{y}^2)$.

McGehee coordinates (q,p,θ,ω) near infinity:

$$x + \mathrm{i}\, y = \frac{2}{q^2} e^{\mathrm{i}\,\theta}, \qquad \dot{x} + \mathrm{i}\, \dot{y} = \left(p + \mathrm{i}\left(q^2\omega/2 - 2/q^2\right)\right) e^{\mathrm{i}\,\theta}.$$

If α is the argument of the massless body in sidereal $(X_1 = r\cos(\alpha), X_2 = r\sin(\alpha))$ then $\theta = \alpha - t$.

One can derive the ODE for (q,p,θ,ω). In particular, for a fixed C there is a **periodic orbit at** ∞, OP_∞ with $q = 0, p = 0, \omega = C/2, \theta \in \mathbb{S}^1$, $\dot{\theta} = -1$. As q goes to (or away) from ∞ as $\pm(8/9)^{1/4} t^{-1/3}$ (from Kepler) it is **parabolic in the DS sense**.

We look for a **local expression of W^s_∞**, for $q > 0$ small, of the form

$$p = F(q,\theta) = \sum_{j\geq 1} a_j(\theta) q^j = q + \ldots,$$

where $a_j(\theta)$ are periodic functions in θ. Using the **symmetry** $(q,p,\theta,\omega,t) \to (q,-p,-\theta,\omega,-t)$, we have $p = -F(q,-\theta)$ **for W^u_∞**.

The $a_j(\theta)$ can be computed in a recurrent way and we obtain

$$p = q - \frac{C^2}{2^5} q^3 + \left(\frac{\mu(1-\mu)}{2^5} - \frac{C^4}{2^{11}} \right) q^5 + \frac{9\mu(1-\mu)}{2^7} \sin(2\theta) q^8 + \ldots,$$

which can be easily extended to high order.

If $\mu = 0$ then $W^{s,u}_\infty$ are given as $p = \pm q\sqrt{1 - q^2 C^2/16}$, i.e., **the manifolds coincide**. In particular $W^s_\infty \cap \Sigma = W^u_\infty \cap \Sigma$ is a **circle of radius** $q = 4/C$. The points in Σ with $q < 4/C$ correspond to **elliptic** orbits of the two-body problem. Points with $q > 4/C$ give **hyperbolic** orbits.

For $\mu > 0$, W^s_∞ and W^u_∞ **do not coincide**. If μ is small enough it is expected that they intersect Σ in **two curves near the circle above**. If $W^s_\infty \cap \Sigma$ is given by $q = 4/C + g^s(\theta;\mu,C)$ (in polar coordinates) then $W^u_\infty \cap \Sigma$ is given by $q = 4/C + g^u(\theta;\mu,C)$ with $g^u(\theta;\mu,C) = g^s(-\theta;\mu,C)$.

In particular these curves intersect at $\theta = 0$ and $\theta = \pi$ giving rise to orbits which **escape parabolically to infinity for $t \to \pm\infty$**.

Note that $W^{s,u}_\infty$ are **analytic with analytic dependence on parameters on a suitable compact** in an open set around $q = 0, p = 0$, **except at the origin itself**.

We also remark that in present case we deal with the invariant manifolds of a **parabolic object** (in the Dynamical Systems sense). This produces changes in the expression of the **return time** and, hence, in the related **separatrix and standard**-like maps.

To obtain $g^s(\theta;\mu,C)$, let $\mathbf{z}=(q,p,\theta,\omega)$ and then **proceed as follows**:

1) **write** $\dot{\mathbf{z}} = F_0(\mathbf{z}) + \mu F_1(\mathbf{z}) + F_2(\mathbf{z},\mu), \quad F_2 = \mathcal{O}(\mu^2)$,

2) look for **initial conditions** $\mathbf{z}_i = \mathbf{z}_0 + \mu(\Delta q, 0, 0, \Delta\omega) + \mathcal{O}(\mu^2)$ where $\mathbf{z}_0 = (4/C, 0, \theta_0, C/2)$ such that the solution $\mathbf{z}(t;\mathbf{z}_i,\mu)$ **belongs to** W^s_∞. Note that for C fixed, $C \neq C_c$, Δq and $\Delta\omega$ are not independent,

3) set $\mathbf{z}(t;\mathbf{z}_i,\mu) = \mathbf{z}(t;\mathbf{z}_0,0) + \mu\mathbf{z}_b(t;\Delta q) + \mathcal{O}(\mu^2)$, with $\mathbf{z}(t;\mathbf{z}_0,0)$ **solution of the 2BP** and $\mathbf{z}_b$ of the **variational problem**
$$\dot{\mathbf{z}}_b = DF_0(\mathbf{z}(t;\mathbf{z}_0,0))\mathbf{z}_b + F_1(\mathbf{z}(t;\mathbf{z}_0,0)), \quad \mathbf{z}_b(0) = (\Delta q, 0, 0, \Delta\omega).$$

To carry out the computations it is convenient to introduce a **new time** τ through $dt/d\tau = C/\hat{q}^2$, $\hat{q}$ being the first component in the 2BP.

Let $g_c^s(\mu, C)$, $g_e^s(\theta; \mu, C)$, $g_o^s(\theta; \mu, C)$ be the **average and the even and odd parts of the purely periodic terms wrt θ, of $\mu\Delta q + \mathcal{O}(\mu^2)$**.

Note that, due to symmetry properties, the **splitting** will be $g^u - g^s = -2g_o^s(\theta; \mu, C)$.

Lemma. If C **is large enough**, then

1. $g_c^s(\mu, C) = \mu \left(\frac{32}{C^5} + O_9 \right) + \mathcal{O}(\mu^2)$,

2. $$g_e^s(\theta_0; \mu, C) = \mu \left[\cos(\theta_0) \left(\frac{3{\cdot}2^{18}}{C^{13}} + O_{16} \right) + \cos(2\theta_0) \left(-\frac{9{\cdot}2^{12}}{C^{11}} + O_{14} \right) + \ldots \right] + \mathcal{O}(\mu^2),$$

3. $$g_o^s(\theta_0; \mu, C) = \mu \left[\sin(\theta_0) \exp(-C^3/24) \left(-\frac{\sqrt{\pi}}{16} C^{1/2} + \ldots \right) + \sin(2\theta_0) \exp(-C^3/12) \left(\frac{\sqrt{2\pi}}{4} C^{5/2} + \ldots \right) \right] + \mathcal{O}(\mu^2),$$

where O_k stands for terms of order k in C^{-1}.

Let Q be the distance to the pericenter, shifted by g_c and g_e. Deriving **suitable separatrix and standard maps** we obtain a bound for the location of the **outermost IRC** for μ **small and** C **large**

$$Q_0 \geq \left(\frac{3}{\kappa_G}\right)^{2/5} \frac{\pi^{3/5}}{8} C^{4/5} \mu^{2/5} \exp(-C^3/60).$$

We can write

$$g^s(\theta) = g_c^s + g_e^s + g_o^s, \qquad g_e^s = \sum_{j>0} c_j \cos(j\theta), \qquad g_o^s = \sum_{j>0} s_j \sin(j\theta)$$

and we must consider some

Remarks

a) The terms $\mathcal{O}(\mu^2)$ are neglected in the Lemma. It can not be excluded that there appear **terms containing** $\mu^2 \exp(-C^3/24)$ **as a factor**. They will be **larger** than the terms in $\mu \exp(-C^3/12)$ provided μ is not very small. In fact this **do happens**.

b) Computing $\mathbf{z}_b$ we have taken out the factor μ. Due to **symmetry reasons** we should take also out a **factor** $1-\mu$. This is relevant for μ **not small**. If $\mu = 1/2$ **the problem is** π**-periodic** and **odd harmonics become zero**.

c) For large C and μ away from $1/2$ the **dominant term in the splitting is** s_1. The function $g_o^s(\theta)$ can even be **wild** and contain harmonics of similar amplitude. This affects also the number of **primary homoclinic points** for $\theta \in [0, 2\pi)$, beyond the obvious ones located at 0 and π.

For **numerical checks** W^s is computed **near** $q = 0$ from **high order local expansions** for suitable q and 2^{12} equispaced θ values. Then **a high order Taylor method** is used until Σ $(p = 0)$ **keeping the values of** θ **and** $g^s(\theta) = q - 4/C$. These values are **Fourier analyzed**.

Based on the previous **remarks** we introduce suitable **scaling factors** to **check against theory**:

For the **computed coefficients** g_c, c_1, c_2

$$\hat{g}_c = \frac{C^5}{\mu(1-\mu)} g_c, \quad \hat{c}_1 = \frac{C^{13}}{\mu(1-\mu)(1-2\mu)} c_1, \quad \hat{c}_2 = \frac{C^{11}}{\mu(1-\mu)} c_2$$

For the **computed coefficients** s_1, s_2

$$\hat{s}_1 = \frac{-s_1 \exp(C^3/24)}{\mu(1-\mu)(1-2\mu)\sqrt{\pi C}/16},$$

$$\hat{s}_2 = \frac{s_2 \exp(C^3/12)}{\mu(1-\mu)C^{5/2}\sqrt{2\pi}/4}, \quad \hat{s}_2^* = \frac{s_2 \exp(C^3/24)}{(\mu(1-\mu)(1-2\mu))^2},$$

where $\hat{s}_2$ is only used for $\mu = 1/2$ and $\hat{s}_2^*$ only for $\mu < 0.45$).

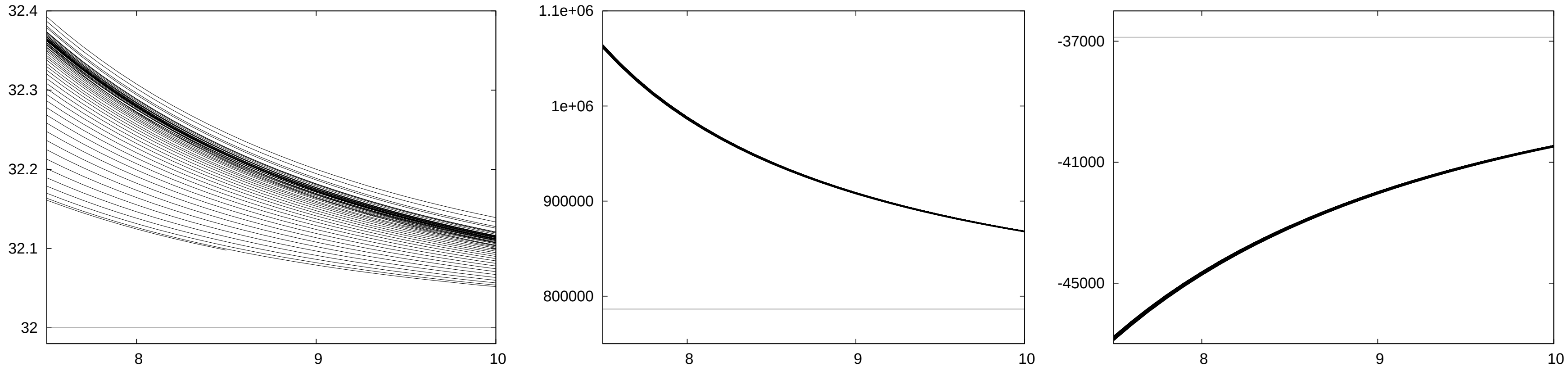

Values of $\hat{g}_c, \hat{c}_1$ and $\hat{c}_2$ (left, middle, right) as depending on C. All μ values are plotted together. Horizontal lines: theoretical limits.

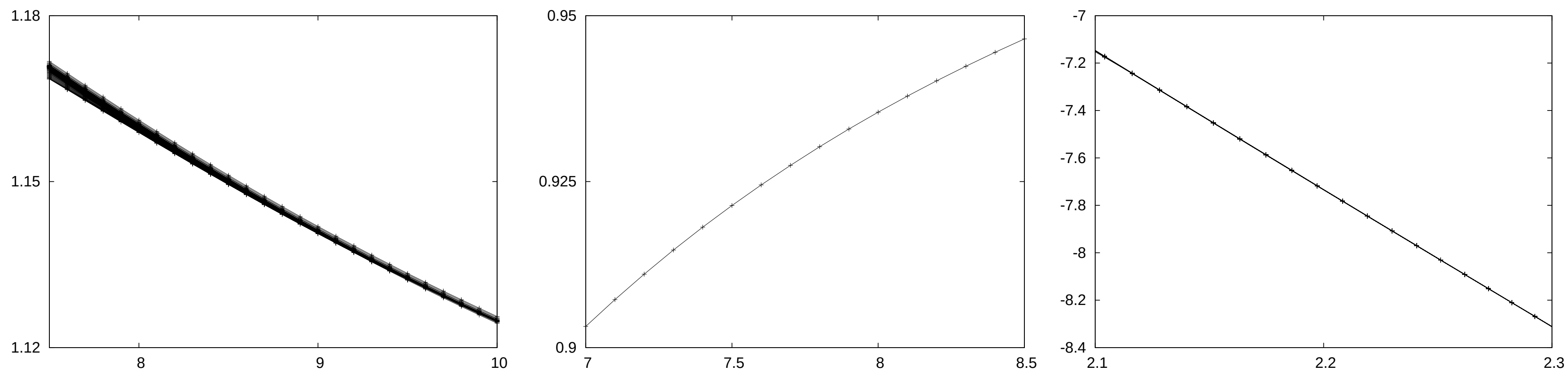

Left and middle: Plots of the scaled $\hat{s}_1$ and $\hat{s}_2$ as functions of C. Should tend to 1 when $C \to \infty$. Right: $\log(\hat{s}_2^*)$ as a function of $\log(C)$. It shows a clear close to linear behaviour $\approx \log(240) - 6\log(C)$ from a linear fit.

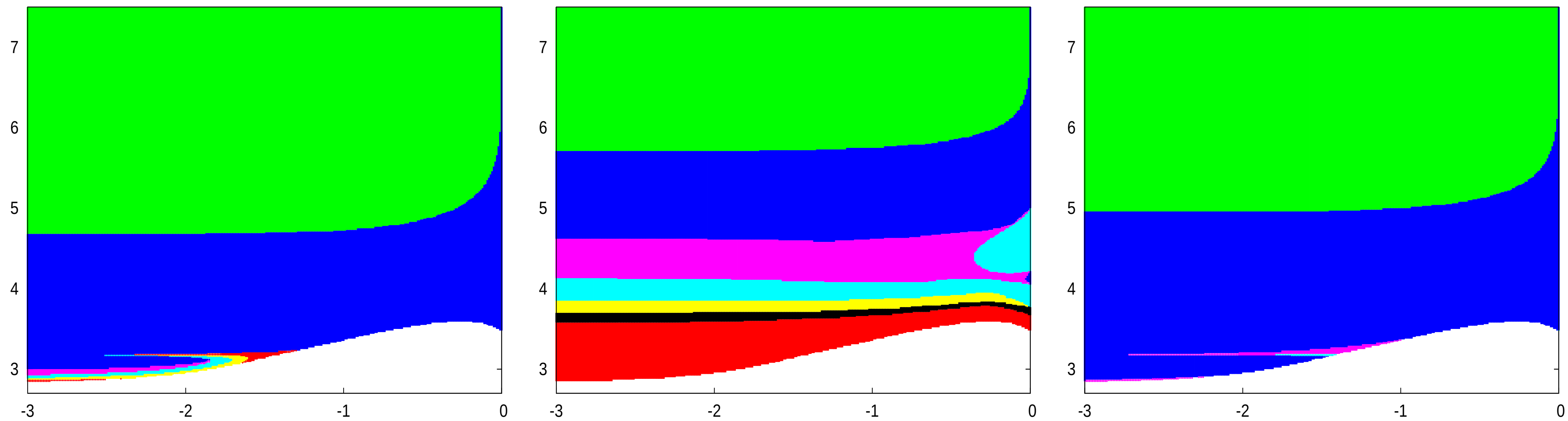

Different characteristics of the **splitting function** as a function of the variables $(\log_{10}(2\mu), C)$. Left: the **dominant term** s_k in the splitting. Middle: **number of relevant harmonics** needed to have a good approximation to the function. Right: the number of zeros, i.e., **primary homoclinic points**.

Color codes.

Left: green, blue, magenta, light blue, yellow, red for $k = 1, 2, 3, 4, 5, > 5$.

Middle: green, blue, magenta, light blue, yellow, black, red for $k = 1, 2, 3, 4, 5, 6, > 6$.

Right: green, blue, magenta, light blue for $k = 2, 4, 6, 8$.

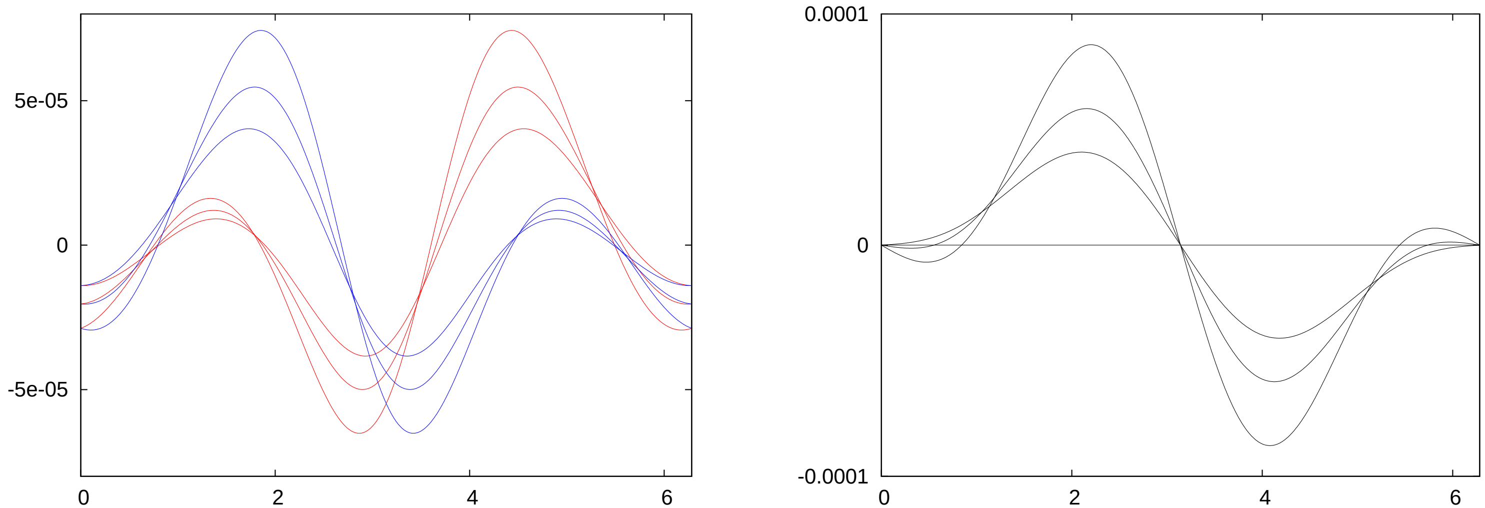

The vicinity of the **bifurcation from 2 to 4 zeros** for the splitting function for $\mu = 0.5 \times 10^{-1.7} \approx 0.0099763$ and $C = 5.0, 4.9, 4.8$. Left: The functions $g^s - g_c$ (red) and $g^u - g_c$ (blue). Decreasing C the value of these functions on $\theta = 0$ decreases. Right: The corresponding **splitting functions**, with 2 zeros for $C = 5.0$ and 4 for $C = 4.9, 4.8$.

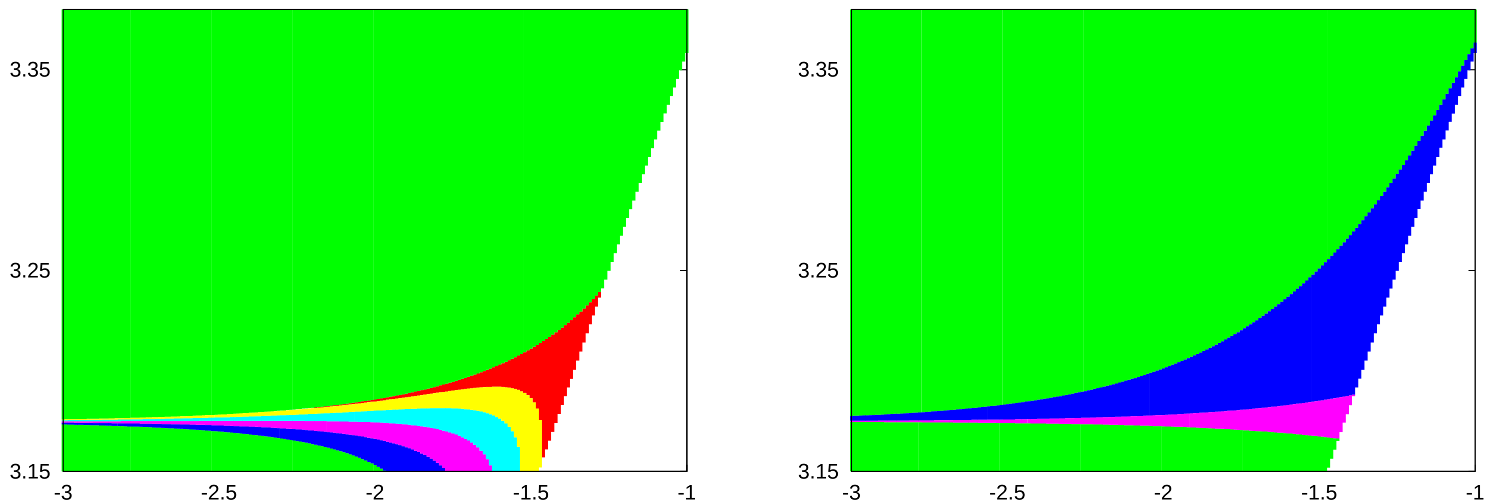

Results in a **vicinity of the critical C_c value** (≈ 3.1748021039364).
Left:
Magnification of the plot concerning the **dominant harmonic** s_k. The color code is now: green, blue, magenta, light blue, yellow and red for $k = 2, 4, 5, 6, 7$ and > 7, respectively. The white zone corresponds to places where g^s is not a graph wrt θ.
Right:
The **number of zeros** of the splitting function, where green, blue and magenta denote 4, 6 and 8 zeros, respectively.

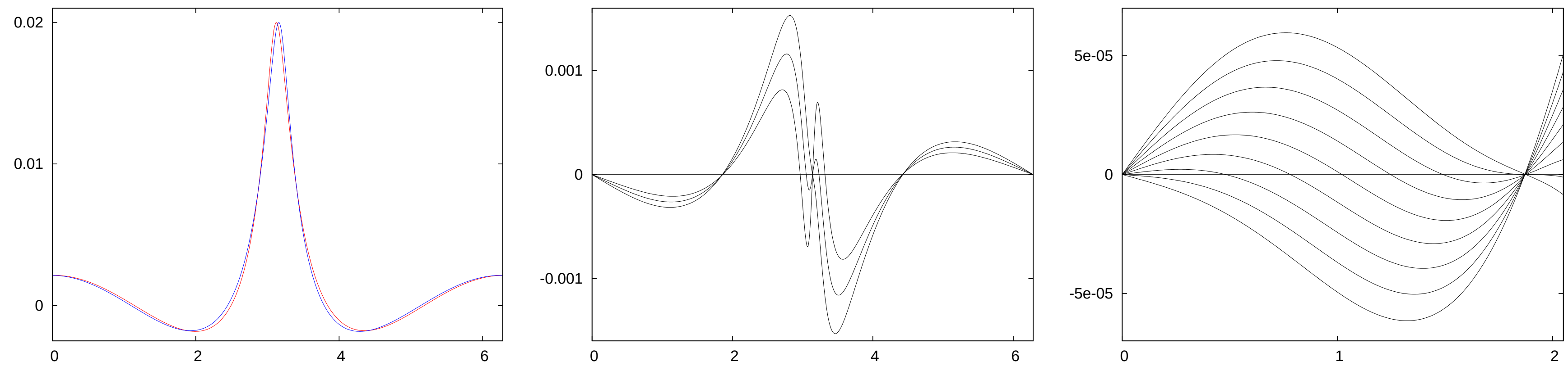

Several phenomena for **small** μ equal to $0.5 \times 10^{-1.7}$ and different C.
Left: g^s (blue) and g^u (red) for $C = 3.2$, displaying a **sharp peak**.
Middle:
The **splitting** function $-2g_o^s$ for $C = 3.23, 3.22$ and 3.21. The absolute maxima decrease with C. Between 3.23 and 3.22 the number of zeros changes from 4 to 6.
Right:
Part of the splitting function for $C = 3.168(0.002)3.184$. When C decreases the value at $\theta = 1$ increases. For $C \in (3.180, 3.182)$ a **new zero emerges** for $\theta \approx 0$ (and the symmetric one near 2π), going from 6 to 8 zeros. It moves to the right by decreasing C until **3 zeros coalesce** and only 1 remains. The situation is symmetrical for $\theta > \pi$, then going from 8 to 4.

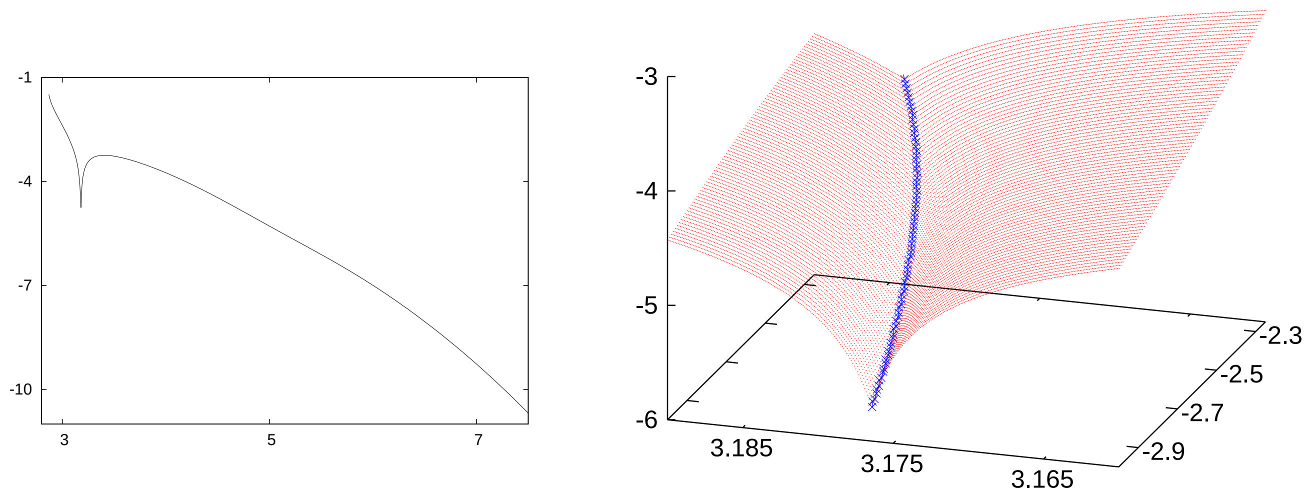

Evolution of the **maximal amplitude** of g_o^s (and, hence, of the splitting function) for **fixed μ by changing C**.
Left:
For $\mu \approx 0.0012559$ the $\log_{10}$ of this amplitude is shown as a function of C.
Right:
Evolution of the local minima in the (μ, C) plane in a 3D plot. The variables shown are $\log_{10}(2\mu)$ (in $[-3, -2.25]$), C (in $[3.16, 3.19]$) and the $\log_{10}$ of the amplitude. The location of the minima, marked in blue, shows that for **$\mu \to 0$ one has $C \to C_c$**.

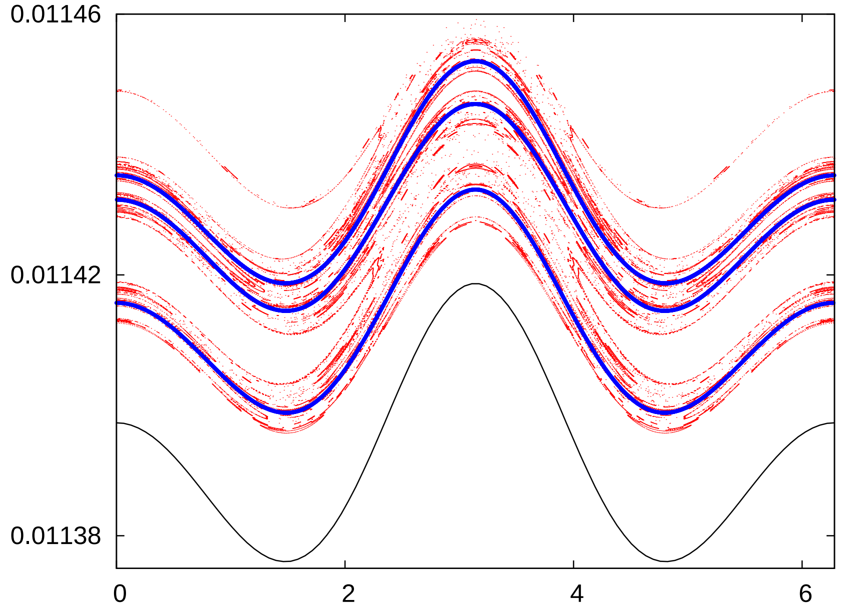

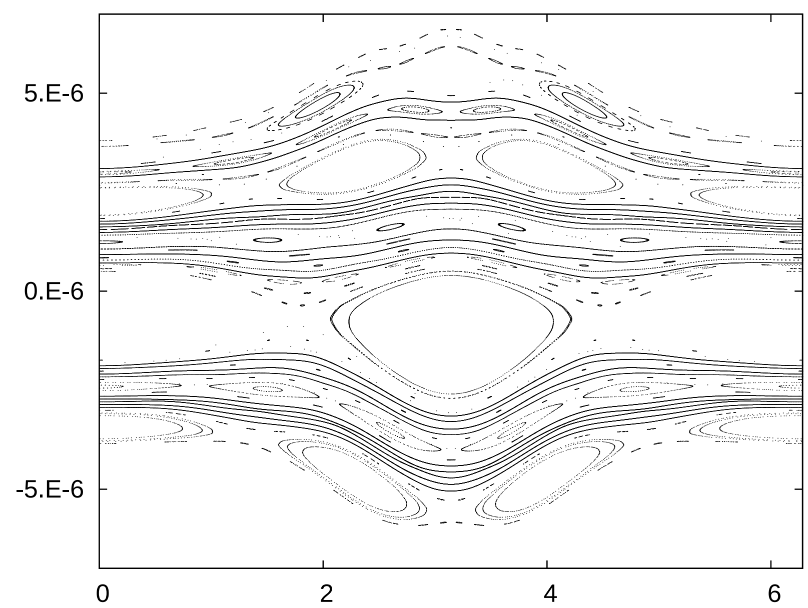

Parameter values $\mu = 0.1, C = 6$.

Left:

An example of **iterates of orbits of the Poincaré map** associated to Σ (pericenter passage), including some of the **first IRC** (the ones with minimal Q) found in that case. Variables plotted: $(\theta, Q = 4/C - q)$.

A plot of $g_c + g_e^s(\theta)$, shifted up by 0.01177, is also shown in black.

Right:

The **dynamics in one the "layers"** modified to skip the large oscillations that affects them. Reminiscent of the **layers in a standard-like map**.

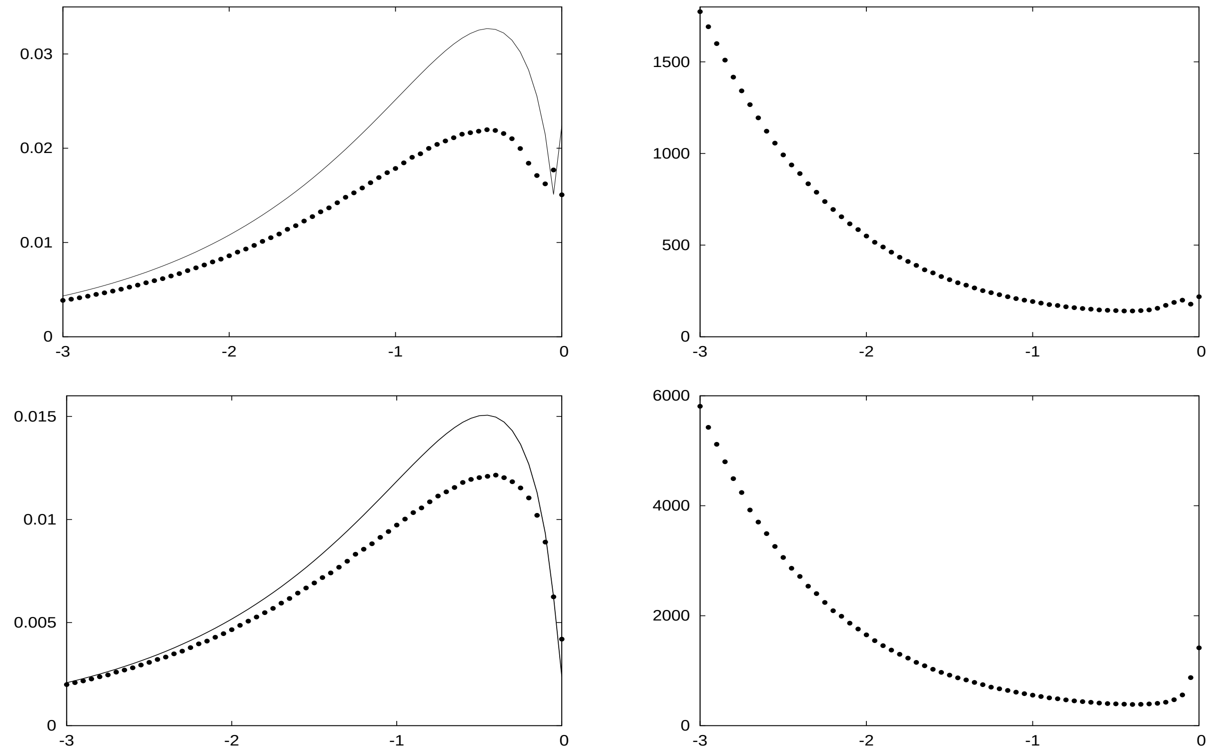

Places where **IRC start to be found**. Horizontal variable: $\log_{10}(2\mu)$.
Up: for $C = 5.5$. Down: for $C = 6.0$.
Left: Values of Q as a function of μ. The **continuous** lines show the **theoretical** values based on a classical **standard map** approximation.
Right: Values of the **average return time to** Σ, $T(Q)$, measured in revolutions of the primaries.
The computations use a combination of **detection of islands** and estimates of **Lyapunov exponent and rotation number**.

Summarizing:

We have shown how one of the tools of Dynamical Systems, the return maps, allows to make predictions on some global properties of a system.

Beyond contributions to integrability, manifolds, splitting, return maps, periodic orbits, invariant tori, homoclinic and heteroclinic phenomena, strange attractors, diffusion, statistical properties, etc, in different general models, the UB-UPC team has considered concrete applications.

They include topics in astrodynamics (design and control of space missions), astronomy, astrophysics, fluid mechanics, Schrödinger equation, atmospheric models, atomic physics, biology, etc, including the required symbolic and numerical tools, when required.

Thanks for your attention